J Solid State Electrochem (2004) 8: 778–785
DOI 10.1007/s10008-004-0545-6

ORIGINAL PAPER

**Elena V. Timofeeva · Marina I. Borzenko
Galina A. Tsirlina · Evgeny A. Astaf'ev · Oleg A. Petrii**

Mutual indirect probing of platinized platinum/tungstate nanostructural features

Received: 21 March 2004 / Accepted: 10 April 2004 / Published online: 14 August 2004

Abstract The comparative study of isopolytungstates immobilized on smooth Pt and platinized Pt (Pt/Pt) provides a possibility to separate several specific effects on H- and O-upd at an external platinum surface and inside the pores of Pt/Pt. In the former case, a solid rechargeable product is formed (nonstoichiometric tungsten bronze), which an inherent porous structure allows solution penetration and does not prevent charging of the Pt/solution interface. Electrochemical responses of smooth Pt give more precise information on the film behaviour, when adsorption phenomena are clarified on the basis of data for Pt/Pt. Electrocatalytic tests (nitrate reduction) confirm unambiguously that the major part of the internal Pt/Pt surface area is modified by adsorbed polytungstate. This result gives, in its turn, new understanding of the size of Pt/Pt pores on the nanometre scale.

Keywords Isopolytungstates · Tungsten bronze · Rechargeable films · Cyclic Voltammetry · Scanning tunneling microscopy

Introduction

Electrochemistry of conductive inorganic solids is an attractive and thriving research area at the border of material science and electrochemistry. The style of Galus's scientific school as applied to this area [1, 2, 3] demonstrates high-level examples of combining various electrochemical techniques for self-consistent studies of electrodeposition and characterization of solids. An attempt to apply a similar combination to the study of an oxometalate-based system is presented here.

Catalysis by oxometalates (in particular, oxotungstates) immobilized at the interfaces (both 2D and 3D layers) form several fields [4, 5, 6, 7, 8, 9, 10, 11, 12, 13] in which the number of promising findings is as much as the number of still unclear mechanisms. One of these fields is electrocatalysis by oxometalates, and the majority of electrocatalytic data correspond to oxometalates immobilized on carbon supports.

The broadly understood concept of mediator mechanisms (electron-transfer mediation or complex formation) basically looks realistic for many systems. However, there are also some examples of catalytic effects [14, 15, 16], which can be hardly explained uniquely by this type of mechanism and which are more consistent with bifunctional mechanisms or third-body effect. Usually these intriguing effects are observed when metallic platinum and oxometalates coexist at the surface.

The specific feature of polyoxometalates is their large molecular size (usually exceeding 1 nm) comparable with typical nanostructural sizes of catalysts of high surface area. As highly dispersed materials are uniquely of interest for electrocatalytic applications, we are sure that one should combine the mechanistic electrocatalytic studies of smooth modified electrodes with special testing of dispersed materials.

We consider a platinum support as not only being of interest for any type of model bifunctional catalysis, but also as a very useful system for understanding the surface location/properties of isopolytungstate species. In this study we succeeded in exploiting the effects of isopolytungstate surface modification on H-and O-upd on smooth polycrystalline and platinized platinum for extracting information about the surface distribution of the resulting oxotungstate species along the surface of porous platinum. Simultaneously we were able to recognize some important structural features of platinized platinum (Pt/Pt) which are of general interest for electrocatalysis on modified surfaces and contribute to

Dedicated to Zbigniew Galus on the occasion of his 70th birthday

E. V. Timofeeva · M. I. Borzenko (✉) · G. A. Tsirlina
E. A. Astaf'ev · O. A. Petrii
Department of Electrochemistry,
Moscow State University, Leninskie Gory 1-str.3,
119992 Moscow, Russia
E-mail: borzenko@elch.chem.msu.ru

further progress in electrochemistry of nanoporous materials.

Recent experiments [17] demonstrated the specific features of Pt/Pt fabricated in polytungstate-containing solutions. Here we consider an alternative two-step modification, namely deposition of isopolytungstates on already prepared Pt/Pt. We use the original deposition procedure [18] consisting in cathodic electrocrystallization of $H_xWO_3{\cdot}nH_2O$ bronze from metastable long-lived acid solutions of isopolytungstates. A 3D film of this material on smooth platinum undergoes quasiequilibrium recharging at the potentials of the H-upd region, consisting in partial W(VI/V) reduction [19]. This material is believed to be similar to well-known catalytically active films formed on non-noble surfaces at high negative potentials [21], but with a much lower number of reduced tungsten atoms.

Materials and methods

The reagents $Na_2WO_4{\cdot}2H_2O$ and 18 M H_2SO_4 were of analytical grade quality (Merck). Twice-distilled water was additionally purified using a Milli-Q setup. High-purity-grade $H_2PtCl_6{\cdot}H_2O$ (Reakhim, Russia) was used for platinization. All data were obtained for 0.5 M H_2SO_4 supporting solution. The model reactants for electrocatalytic tests were potassium nitrate and sodium nitrite (Reakhim, Russia) twice recrystallized from bidistilled water.

To prepare long-lived sulfuric acid solutions of isopolytungstate we used $Na_2WO_4{\cdot}2H_2O$. According to UV–vis spectral data [18], two isopolyanions ($[W_7O_{24}]^{6-}$ and $[W_{10}O_{32}]^{4-}$) predominate in this deposition solution.[1] The necessary sodium tungstate portion was placed into a flask, water was added (about 80% of the final solution volume), and the flask was heated. When boiling started, and the substance had completely dissolved, then the required amount of 18 M H_2SO_4 was rapidly added into the hot tungstate solution (protective measures were necessary to avoid the flask cracking), and finally the solution level was adjusted to the mark with water.. Details of the film preparation are presented in Ref. [19]. In the course of preparation, the equilibrium in the deposition solution bulk shifts little by little towards the formation of an insoluble product (tungstic oxide). The possibility to stabilize W(VI) in acid by using similar procedure was reported earlier [22], but any solutions used by other authors to deposit solid WO_x were always prepared by other techniques, namely metallic tungsten dissolution in H_2O_2-containing acid [12].

A 0.2-mm-thick platinum foil was used directly or after platinization. Platinum was deposited potentiostatically from 10 mM H_2PtCl_6 and 0.5 M H_2SO_4 solution as described in Ref. [9]. Roughness factors (R_f) were determined experimentally from H-upd according to the conventional technique [23]. The weight of the deposits was calculated from the deposition charge and corrected for 90% current efficiency [23]. The specific surface area after potentiodynamic ageing [23] amounted to 10–16 $m^2\ g^{-1}$, which is a typical value for the deposition mode applied [24]. All charge and current densities are reported here for the real surface area, if there is no special indication.

Cyclic voltammograms (CVs) were measured with scan rates of 5–100 mV s^{-1} using an EG&G PAR model 173 potentiostat/galvanostat equipped with a model 175 universal programmer and a model 179 digital coulometer or an EG&G PAR model 273 device. Stationary polarization curves of nitrate electroreduction were measured potentiostatically like in Refs. [25, 26, 27, 28]: any time after the application of a potential step the current transient was recorded, and the stationary current value was determined; this differed from the previous value by less than 1% per minute. Usually it took about 15 min to attain the stationary value using this criterion. The current values reported in Refs. [25, 26, 27, 28] are slightly less stationary, but the estimated difference does not exceed 10%.

Three-electrode cells with separated compartments and RHEs in the same solution were used in all experiments. Before the experiment, the solutions were bubbled with argon for 30–60 min. All potentials are reported using the RHE scale.

Scanning tunnelling microscopy (STM) images of modified electrodes were obtained by using a LitScan-2 homemade device, typically under constant current mode (about 200 pA), with a tunnelling voltage of about 300 mV. The specific features of Pt/Pt imaging are discussed in Refs. [23, 29].

Results and discussion

The modification procedure described in Ref. [18] for smooth platinum foil was extended to Pt/Pt electrodes with relatively low roughness (R_f of about 100). We avoided higher roughness at this stage because only for the deposits of submicron thickness has the detailed structure been characterized [24].

For both smooth platinum and Pt/Pt, cyclic treatment in isopolytungstate solution (Fig. 1) results in an increase of charge in the H-upd region (Q_H).[2] For any certain cycle number, the former effect is more pronounced for smooth platinum (Fig. 1b). A simultaneous decrease of charge in the O-upd region (Q_O) takes place, and looks similar for both materials. An additional

[1] The latter anion is reduced at positive potentials (reference hydrogen electrode, RHE, scale) [19], in contrast to other isopolytungstates [20], where reduction is accompanied by hydrogen evolution

[2] We use "H-upd" here simply to indicate the potential region. H subscript has the same meaning, i.e. Q_H should be understood as the total charge in the H-upd region, not as the charge spent for hydrogen desorption

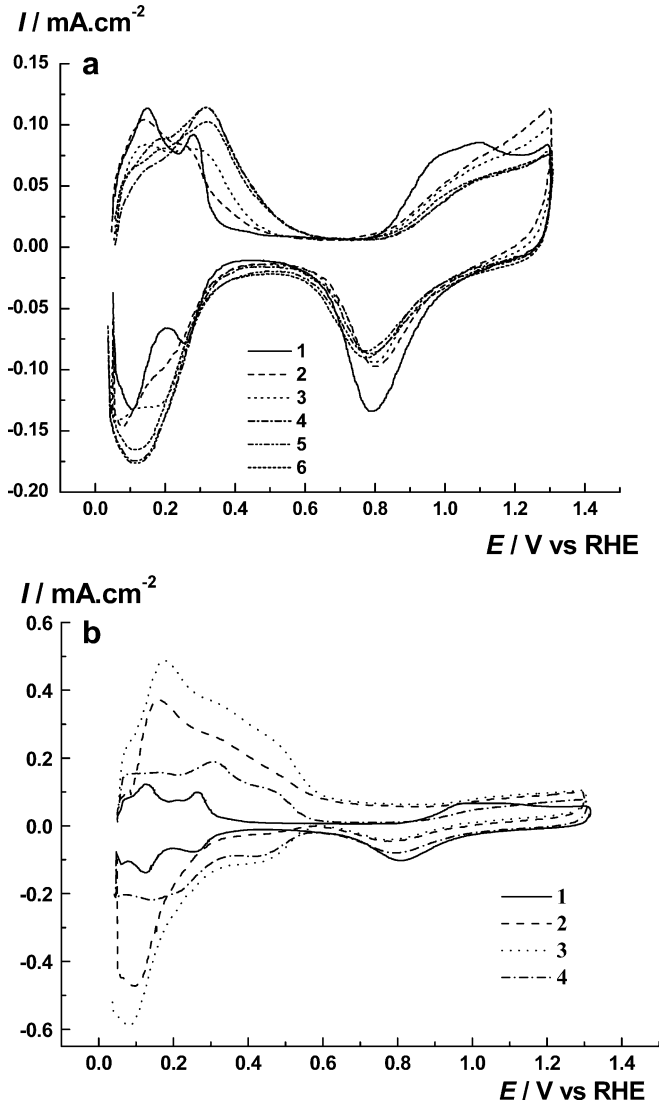

Fig. 1 Cyclic voltammograms of **a** platinized Pt (*Pt*/*Pt*) ($R_f = 56$) and **b** Pt foil ($R_f = 2.8$) in 0.5 M H_2SO_4 solution (*curves 1*, **a** *curve 6*, **b** *curve 4*) and in 0.5 M H_2SO_4 plus 1 mM Na_2WO_4 modification solution (**a** *curves 2–5*, **b** *curves 2, 3*). Curves 1 before modification; **a** curve 6 and **b** curve 4 after modification. Cycle numbers in the course of modification: curves 2 1; **a** curve 3 3, curve 4 40, curve 5 100; **b** curve 3 100. Scan rate 100 mV s^{-1}

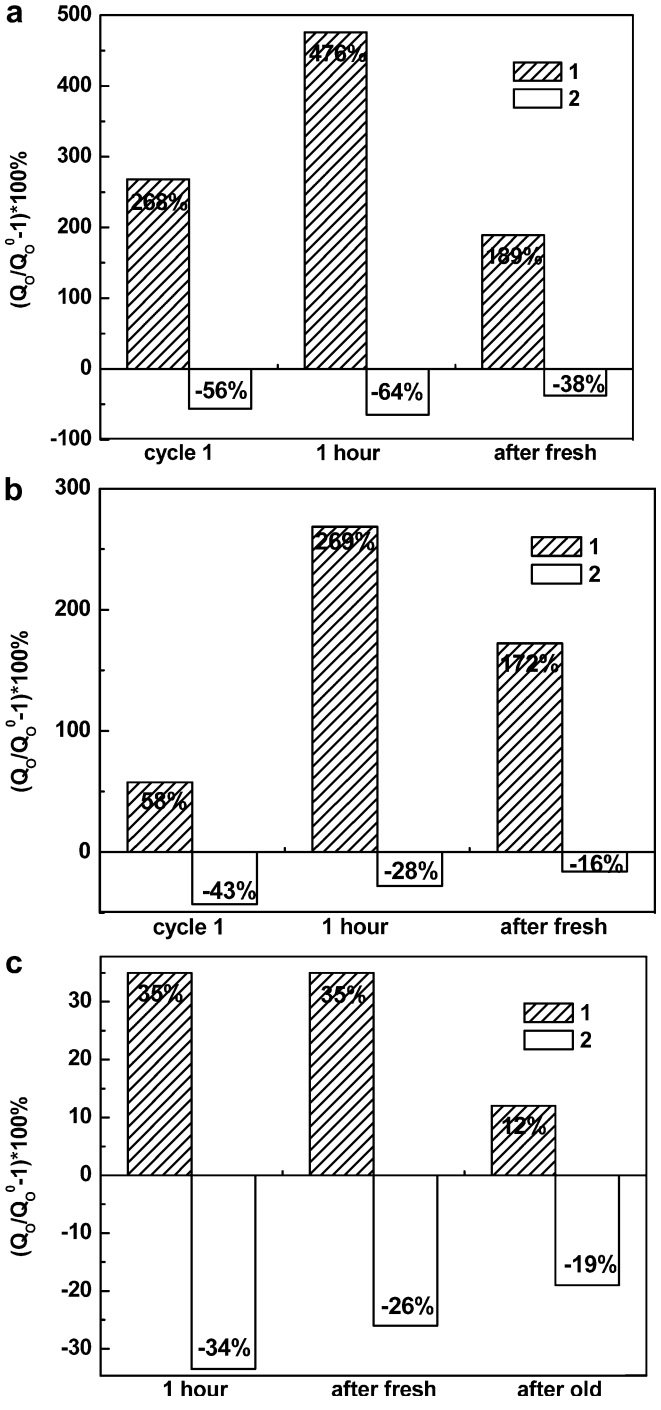

Fig. 2 Comparative representation of Q_H (*dashed areas*) and Q_O (*empty areas*) changes at various deposition stages for **a**, **b** smooth Pt and **c** Pt/Pt. The difference between **a** and **b** consists in the deposition mode (with or without delay at 0.05 V for 35 s)

specific feature of smooth platinum behaviour in the solution under study is the increase of current in the overall double-layer region (for Pt/Pt it was observed only at $E < 0.6$ V).

We have already demonstrated [18] that there are two redox-processes taking place simultaneously in isopolytungstate solution: reversible redox W(VI/V) reaction with participation of soluble species and W(VI) reduction with formation of a rechargeable solid product which remains at the surface after washing. As the former process, the formal potential of which was estimated as $E(\mathrm{RHE}) = 0.14 \pm 0.05$ V [18], is diffusion-controlled, its rate is proportional to the geometrical surface area. Correspondingly, its contribution to the CV of Pt/Pt is negligible. This circumstance makes it easier to monitor other phenomena taking place in the course of cycling.

The changes of Q_H and Q_O at various deposition stages and the resulting changes after deposition (data for freshly deposited films; for Pt/Pt data for aged films are also included) are compared in Fig. 2. The latter are always lower, at least for Q_H, because the essential increase of Q_H in the deposition solution results from the

contribution of the redox process with participation of soluble isopolytungstate species. Figure. 2a and b illustrates the role of delay at the cathodic potential limit, which favours the accumulation of rechargeable solid product.

For smooth platinum, both the increase in Q_H and the decrease in Q_O with cycle number are monotonic. For Pt/Pt more complex correlation of Q_H and Q_O (Fig. 3a) was observed, which points out the interplay of several phenomena. Three regions can be marked out:

1. Very few initial cycles, with a sharp decrease of charge for O-upd and a fast increase of charge in the hydrogen region.
2. Two dozen intermediate cycles, in which the charge for O-upd continues to decrease, while the charge in the hydrogen region demonstrates minor changes.
3. All subsequent cycles, in which there are practically no changes of O-upd with simultaneous continued growth of charge in the H-upd region.

For Q_O there are no specific features compared with smooth platinum (Fig. 3b). Nonmonotony in a few initial cycles comes from Q_H behaviour (Fig. 3c). The behaviour of the current maxima at potentials of weakly and strongly bonded hydrogen differs strongly. For the former, an initial decrease with cycle number is observed, while for the latter, the growth of charge is monotonic. We explain these data as the interplay of polytungstate-induced inhibition of hydrogen adsorption and accumulation of a new rechargeable phase. It was impossible to observe the first phenomenon for smooth platinum because of the much higher redox contribution.

The number of deposition cycles is limited by the stability of the acidic isopolytungstate solution. When the formation of insoluble tungstic acid starts, parallel electrophoretic deposition contributes to solid oxotungstate accumulation. We avoided such situations; and to deposit thicker films we always changed the solution for a fresh one every 1.5–2 h.

The most pronounced difference of smooth platinum and Pt/Pt is observed after washing the electrode and measuring the CV in supporting electrolyte solution (Fig. 1a curve 6, Fig. 1b curve 4). For Pt/Pt, the changes after washing are less pronounced. As one can conclude from Figs. 2 and 3, the stationary degree of O-upd suppression never exceeds 20–40% for both smooth platinum and Pt/Pt, even when the excess charge in the hydrogen region differs up to one order. This means that the film does not prevent completely solution penetration inside porous Pt/Pt. At the same time, a solid film cannot be formed inside the pores because their size is comparable with the lattice parameter of tungsten bronze [30, 31]. So the modification of the internal surface (if any) is possible only with (poly)tungstate (sub)monolayers.

STM evidence of film formation at an external Pt/Pt surface is presented in Fig. 4. The surface morphology

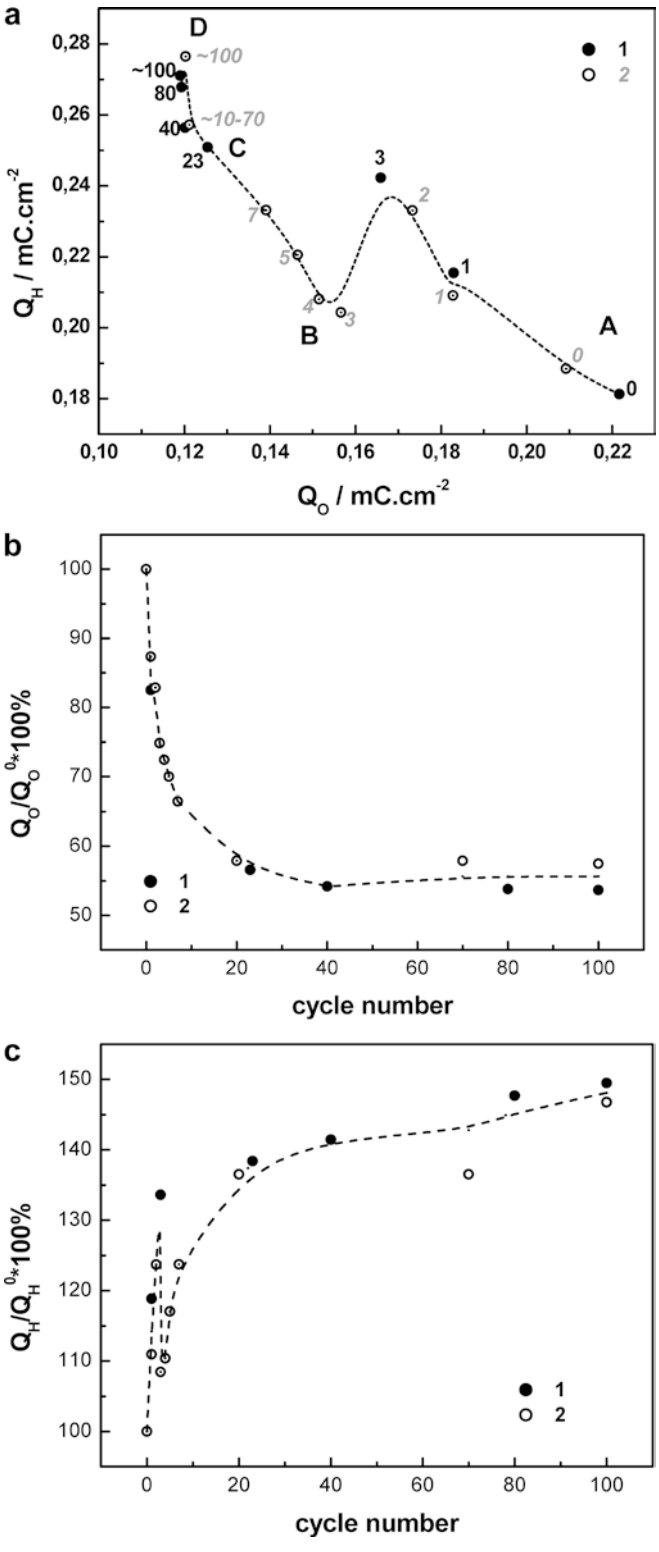

Fig. 3 The coulometric analysis of data for deposition on Pt/Pt: **a** Q_H versus Q_O correlation, and the dependencies of **b** Q_O and **c** Q_H on the cycle number. Data for two electrodes with $R_f = 56$ (*solid symbols*) and 82 (*open symbols*) are presented. All charge values are normalized for the corresponding charges for the bare support (marked with superscript 0). *Capital letters* mark the deposition periods for the samples imaged in Fig. 4

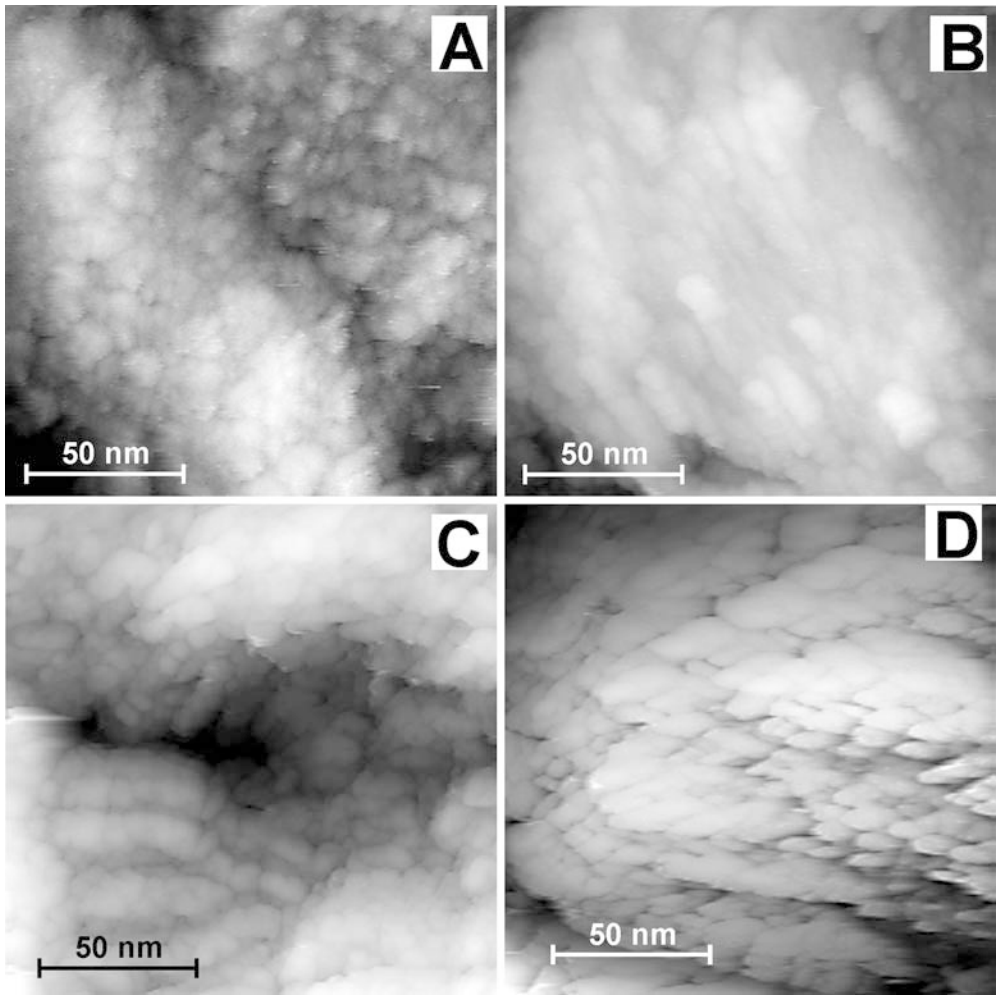

Fig. 4 Scanning tunnelling microscopy (*STM*) images of the surface of Pt/Pt after various numbers of deposition cycles: **a** 0; **b** 4; **c** 25; **d** 100

was imaged by ex situ STM after various periods of electrode modification (corresponding cycle numbers are marked in Fig. 3). As soon as this process took some time, the modification solution was changed after each STM measurement. The typical globular nanostructure of Pt/Pt is given in Fig. 4a; it agrees with previous data [23]. It is demonstrated in Fig. 4b that after four initial cycles there are already two types of surface morphology. The first one is still identical to Pt/Pt [23], but contains fragments of a more-ordered structure. The ordered rows of new solid start to cover all surfaces at higher deposition time (Fig. 4c, d). At this stage there is already a further decrease of oxygen adsorption (Fig. 3b).

The 3D deposit in Fig. 4a and b looks like the film on smooth platinum (images presented in Ref. [18]). It can be concluded unambiguously that the film is easily permeable for solution, because the voltammetric responses confirm oxygen adsorption on a large portion of the real surface of Pt/Pt (including the internal surface). Two explanations can be proposed:

1. Some narrow pores of Pt/Pt are blocked with newly formed solid, and only a portion of the initial true surface area (60–80%) takes part in the O-upd process at the unmodified internal surface.
2. The major part of the internal surface is still available for O-upd, but the properties of this surface are modified by adsorbed (poly)tungstate, and the surface coverage with oxygen at a given potential is lower than on bare Pt/Pt.

Explanation 2 looks more probable because of the similar degrees of O-upd suppression for smooth platinum and Pt/Pt; however, more stronger confirmation comes from the electrocatalytic test.

The ability of adsorbed heteropolycompounds to enhance the reduction of nitrite is widely known, while for nitrate there are no reliable catalytic effects [8]. Nitrate reduction on platinum is a slow process (purely kinetic control) with a region of self-inhibition by hydrogen adatoms [25, 26, 27, 28]. For platinum modified by tungstates two types of catalytic effects can be expected for nitrate reaction. First, the appearance of a parallel mediator pathway is possible. Second, the suppression of H-upd by adsorbed tungstate species, if any, takes place selectively in the region of self-inhibition, and it is possible to prevent this passivation. An example

of the second mechanism is the acceleration of nitrate reduction by foreign adatoms at a certain low coverage of the latter [26]. At higher coverage adatoms suppress not only H-upd, but also the adsorption of nitrogen-containing reactant, and induce inhibition. The permeability of the solid film (tungsten bronze) gives a chance to overcome the latter disadvantage. Electrodes modified with isopolytungstates also look to be possibilities because of the possibility to withdraw them without the loss of the modified layer.

For freshly modified electrodes, a pronounced increase of current in the self-inhibition region was observed, while complete inhibition took place at $E > 0.3$ V (compare curves 1 and 2 in Fig. 5). The same is observed for smooth platinum. This complex catalytic behaviour cannot be related either to blocking effect, or to the presence of a solid film on internal surface, because the activity is proportional to the true surface area. As the current on unmodified platinum is zero in the vicinity of zero RHE potential, so the high activity per true surface area confirms that the internal surface is also modified. This means that isopolytungstate species (or monotungstate species, the concentration in the deposition solution of which is, however, negligible) penetrate into the pores of Pt/Pt. No effect of tungstates on nitrite electroreduction rate was found. This means that we can refer the observed effect (Fig. 5) directly to the initial steps of nitrate reduction.

Ageing of the film results in a decrease of the electrocatalytic effect (Fig. 5, curve 3), but never to its disappearance. The stability of the film in the course of prolonged exposure to working solutions was checked with STM (Fig. 6). Despite some morphological differences there is no doubt that the solid film still exists and does not disappear in the course of the measurements. The film thickness is at least 200 nm (about 250 monolayers of tungsten bronze), as can be estimated using the

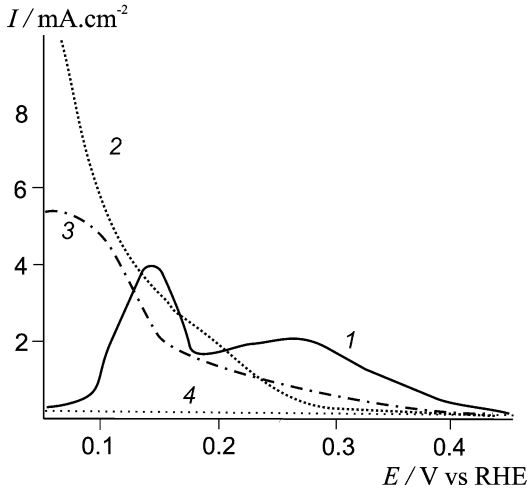

Fig. 5 Stationary polarization curves of nitrate electroreduction measured in 0.5 M H_2SO_4 plus 25 mM KNO_3 solution on Pt/Pt: bare (*1*), freshly modified (*2*), modified and aged (*3*). *Curve 4* corresponds to a blank experiment with isopolytungstate in supporting electrolyte solution

difference of heights in these images. Degradation results preferentially in reorganization of the globular structure. Simultaneous changes of film rechargeability are discussed in Ref. [19].

The extremely complex structure of Pt/Pt and its dependence on the deposition potential are beyond question. Although the attempts to present some Pt/Pt materials as ''well characterized'' look slightly naive, a number of important structural features were determined unambiguously. Namely, the relatively wide size distribution of platinum crystals in the range 2–20 nm was confirmed by both STM imaging [23] and harmonic analysis of precise X-ray diffraction data [24]. Pore size distributions in Pt/Pt materials were studied by means of reference porometry [30, 31]. For freshly deposited 4-μm-thick Pt/Pt, extremely narrow pores with a radius of less than 1 nm were found, which, according to Ref. [30], contribute up to 50% to the real surface area. This result can hardly be considered as having a quantitative meaning, as the possibility to apply the Kelvin equation for the radius versus pressure dependence for these molecular-sized pores looks doubtful. Additional uncertainties probably come from the noncylindrical geometry of the pores, which, if taken into account [32], should decrease the surface-to-volume ratio for the narrowest pores. It should also be mentioned that up to 30% of the true surface area as recalculated in Ref. [30] from porometric data (21 $m^2\ g^{-1}$) does not contribute to the H-upd surface area (for the latter a value of 13.8 $m^2\ g^{-1}$ was reported in Ref. [31]). This means that when referring any adsorption data to H-upd one is dealing only with the pores available for water adsorption.

The key problem is the possibility for large oxotungstate species to penetrate inside the narrow pores. This possibility was discussed as rather questionable even for low molecular anions [31], which demonstrated decreased values of adsorption referred to the H-upd true surface area. The latter result can be explained irrespective of penetration limitations: the decreased equilibrium surface coverage by anions in the pores of low curvature can result from electrostatic reasons and/or the difference in packing geometry. The minimal size of the pores spatially available for oxotungstates can be estimated from adsorption data on zeolites, for which dodecatungstate penetration into the cylindrical pores of 1.5-nm radius has been determined experimentally [33].

For isopolytungstates it is difficult to estimate the size of species because some decomposition–polymerization of oxotungstate fragments in the course of adsorption cannot be ruled out, including the formation of open-chain structures [34]. However, in any case the size of the species hardly exceeds the size of adsorbed dodecatungstate anions (about 1.2 nm [35]). So we can conclude that an oxometalate probe is a very good possibility for analysis of the nanometre-scale porous structure of dispersed platinum, in particular to recognize the portion of the surface inside pores of radius greater than 1.5–2 nm.

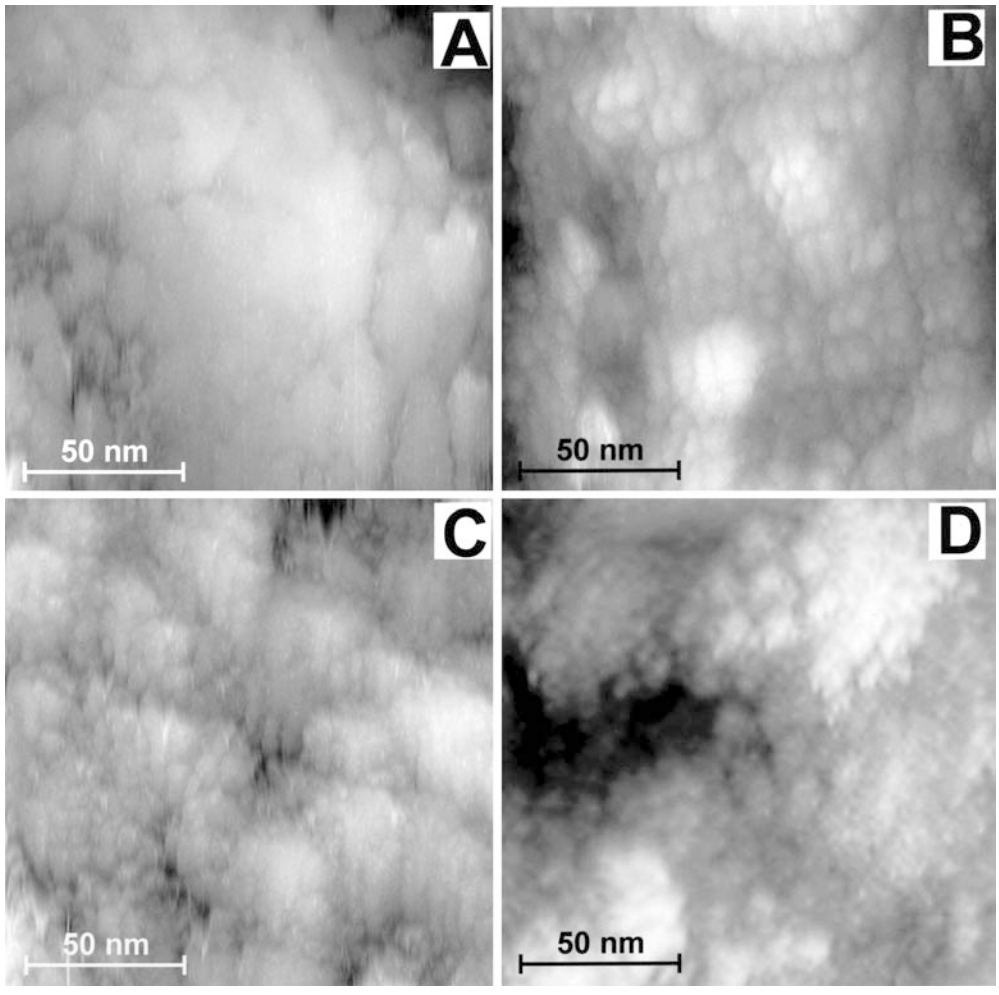

Fig. 6 STM images of a modified Pt/Pt electrode surface: **a** freshly deposited; **b** after 48-h exposure to supporting electrolyte solution; **c** after 48-h exposure to 0.5 M H_2SO_4 plus 25 mM KNO_3 solution; **d** after ageing in air

Conclusions

Parallel electrochemical characterization of smooth and dispersed modified electrodes appeared to favour better understanding of adsorption and electrocrystallization isopolytungstates. Simultaneously it was found that indirect structural tests with polytungstate probes present another interesting application, especially for thicker platinum deposits with pronounced inhomogeneity of the porous structure [24].

To stress the importance of the topic we should also mention that a number of impressive effects were reported for WO_x-containing fuel cell catalysts [36] and polytungstates as fuel cell electrolytes [37]. The appearance of oxotungstate species can also be a reason for anodic activation of tungsten carbide [38] and the high activity of tungsten-containing multimetallic compositions [39]. Tungsten bronze films with known oxygen stoichiometry [19] should be considered as a useful model system to study general phenomena in tungsten-containing catalytic systems.

Acknowledgement We thank the Russian Foundation for Basic Researches, 02-03-33285a.

References

1. Kulesza PJ, Galus Z (1997) Electrochim Acta 42:867
2. Kukulka-Walkiewicz J, Stroka J, Malik MA, Kulesza PJ, Galus Z (2001) Electrochim Acta 46:4057
3. Makowski O, Stroka J, Kulesza PJ, Malik MA, Galus Z (2002) J Electroanal Chem 532:157
4. Kulesza PJ, Faulkner LR (1989) J Electroanal Chem 259:81
5. Keita B, Nadjo L (1989) J Electroanal Chem 258:207
6. Zang X, Chan K-Y, Tseung ACC (1995) J Electroanal Chem 386:241
7. Rong C, Anson FC (1996) Inorg Chim Acta 242:11
8. Sadakane M, Steckhan E (1998) Chem Rev 98:219
9. Jeannin YP (1998) Chem Rev 98:51
10. Klemperer WG, Wall GG (1998) Chem Rev 98:297
11. Nha NV, Ngoc NTB, Hung NV (1998) Thin Solid Films 334:113
12. Granqvist CG (2000) Sol Energy Mater Sol Cells 60:201
13. Bock C, Smith A, MacDougall B (2002) Electrochim Acta 48:57
14. Arico AS, Poltarzewski Z, Kim H, Morana A, Giordano N, Antonucci V (1995) J Power Sources 55:159
15. Shen PK, Chen KY, Tseung ACC (1995) J Electroanal Chem 398:223
16. Tze W, Borzenko MI, Tsirlina GA, Petrii OA (2002) Russ J Electrochem 38:1250
17. Borzenko MI, Chojak M, Kulesza PJ, Tsirlina GA, Petrii OA (2003) Electrochim Acta 48:3797

18. Timofeeva EV, Tsirlina GA, Petrii OA (2003) Russ J Electrochem 39:716
19. Palys B, Borzenko MI, Tsirlina GA, Jackowska K, Petrii OA (2004) Electrochim Acta 49:(in press)
20. Boskovic C, Sadek M, Brownlee RTC, Bond AM, Wedd AG (2001) J Chem Soc Dalton Trans 187
21. Keita B, Nadjo L (1987) J Electroanal Chem 230:85
22. Yu A, Kumagai N, Liu Z, Lee JY (1998) J Solid State Electrochem 2:394
23. Petrii OA, Pron'kin SN, Tsirlina GA, Khrusheva ML, Spiridonov FM (1999) Russ J Electrochem 35:8
24. Plyasova LM, Molina IY, Cherepanova SV, Rudina NA, Sherstyuk OV, Savinova ER, Pron'kin SN, Tsirlina GA (2002) Russ J Electrochem 38:1116
25. Petrii OA, Safonova TY (1992) J Electroanal Chem 331:897
26. Safonova TY, Petrii OA (1998) J Electroanal Chem 448:211
27. Safonova TY, Petrii OA (1998) Russ J Electrochem 34:1137
28. Safonova TY, Petrii OA (1995) Russ J Electrochem 31:1269
29. Vassiliev SY, Pron'kin SN, Tsirlina GA, Petrii OA (2001) Russ J Electrochem 37:448
30. Gladysheva TD, Shkol'nikov EI, Vol'fkovich YM, Podlovchenko BI (1982) Electrokhimiya 18:435
31. Podlovchenko BI, Gladysheva TD, Vyaznikovtseva OV, Vol'fkovich YM (1983) Electrokhimiya 19:424
32. Jena A, Gupta K (2001) J Power Sources 96:214
33. Pamin K, Kubacka A, Olejniczak Z, Haber J, Sulikowski B (2000) J Catal A 194:137
34. Walanda K, Burns RC, Lawrance GA, von Nagy-Felsobuki EI (2000) J Cluster Sci 11:5
35. Lee L, Wang JX, Adzic RR, Robinson IK, Gewirth AA (2001) J Am Chem Soc 123:8838
36. Chen Y, Chen KY, Tseung ACC (1999) J Electroanal Chem 471:151
37. Lavric I, Staiti P, Novak P, Hocevar S (2001) J Power Sources 96:303
38. Tsirlina GA, Petrii OA (1987) Electrochim Acta 32:637
39. Arico AS, Creti P, Giordano N, Antonucci V, Antonucci A, Chuvilin A (1996) J Appl Electrochem 26:959